

Efficient Second Order Fermi Accelerators as Sources of Ultra-High-Energy Cosmic Rays

Tobias Winchen* and Stijn Buitink

Vrije Universiteit Brussel

(Dated: December 13, 2016)

Stochastic acceleration of cosmic rays in second order Fermi processes is usually considered too inefficient to reach ultra-high energies, except in specific cases. In this paper we present the energy spectrum obtained from efficient second order Fermi acceleration in highly turbulent magnetic fields as e.g. found in the outskirts of AGN jets. We parametrize the resulting non- power-law spectra and show that these can describe the cosmic ray energy spectrum and mass-composition data at the highest energies if propagation effects are taken into account.

Cosmic rays are observed with energies from approximately 10 GeV up to energies above 100 EeV with a distribution commonly parametrized as a power-law. The spectral index of the power-law changes at a few certain energies, in particular the ‘knee’ at approximately 1×10^{15} eV and the ‘ankle’ at approx. 5×10^{18} eV. Beyond approx. 4×10^{19} eV the flux is strongly suppressed compared to a simple power-law. The definite origins of cosmic rays and the spectral features knee, ankle, and cut-off are still unknown, but in the prevailing models cosmic rays with the highest energies are of extragalactic origin while cosmic rays with the lowest energies are accelerated in sources within the galaxy (e.g. [1]).

It is typically assumed that the energy spectrum of the cosmic rays at their sources has also to be a single power-law $dN/dE \propto E^{-\gamma}$, maybe with some cut-off at high energies, in order to obtain the power-law observed at Earth (e.g. [2]). A power-law is the result of a statistical acceleration of the particles, when in every acceleration cycle a constant fraction of particles is lost. Notably, acceleration in relativistic shocks via the so called first order Fermi mechanism is considered as an acceleration mechanism that generates a power-law. In the shock acceleration model, a particle traverses a shock front multiple times and is efficiently accelerated, as in every traverse it head-on collides upstream or downstream of the shock. However, this mechanism has some difficulties, as the particles have to return to the shock many times which require special conditions in the shock environment, a high injection energy of the particles into the accelerating region, or multiple shocks [3, 4].

With first order Fermi acceleration, a soft spectral index of the injection power-law of $\gamma \geq 2$ is expected [5]. However, it has been recently recognized by the Pierre Auger Collaboration [6] and others [7–9], that the spectrum and composition data at the highest energies can not be well described by sources with a power-law spectrum with a soft spectral index; instead, hard spectra with $\gamma < 1.5$, or even $\gamma < 0$ depending on the model for the infrared background, are required to fit the data with a single power-law.

These problems do not arise in the original ‘second

order’ acceleration mechanism proposed by Fermi [10], where particles gain energy in collisions with magnetic clouds. Here energy losses are also possible due to tail-on collisions, the average energy gain per collision is only $\Delta E/E = \frac{4}{3}\beta^2$. For velocities of the scatter centers $\beta \ll 1$ this second order acceleration thus requires a large number of scatter events to significantly gain energy. With the originally considered low rate of scatters with slowly moving magnetic clouds at Galactic distances, the mechanism is thus not efficient enough.

To reach the highest energies via a second order Fermi acceleration nevertheless, a high velocity of the scatter centers and/or a low mean free path length between scatter events is required. Such conditions may be found in turbulent magnetic fields; for example, scattering on Alfvén waves in the radio lobes of Centaurus A has been considered [11]. Here, the diffusive propagation of particles that scatter at irregularities $\frac{B}{\delta B}$ of magnetic fields with strength B , is described as random walk. In a field with turbulence spectrum $\frac{k}{k_{\min}}^{-q}$ the mean free path of the particles with energy E and charge Z is

$$\lambda \propto \left(\frac{B}{\delta B}\right)^2 (R_G k_{\min})^{1-q} R_G \equiv \lambda_0 \left(\frac{E}{1 \text{ EeV}} \frac{1}{Z}\right)^{2-q} \quad (1)$$

with gyroradius $R_G = \frac{E}{BZ}$ of the particles [12].

To simulate particle acceleration by magnetic scattering we created a dedicated module within the CRPropa simulation framework [13]. The module scatters the particles into a random direction in the rest-frame of a scattering center moving with velocity β in the laboratory frame after propagating a distance d randomly chosen according to an exponential distribution with mean free-path λ according to eq. 1.

We assume isotropic movements of the cosmic rays and scatter centers in the rest frame of the accelerating region. The distribution of angles θ between the direction of the particle and the scatter center is thus chosen according to $dN/d\theta \propto \theta + \beta \sin \theta$. As head-on collisions are more likely than tail-on collisions, the particle gains on average energy as predicted by second order Fermi acceleration.

The particles are injected with energy E_{inj} into the

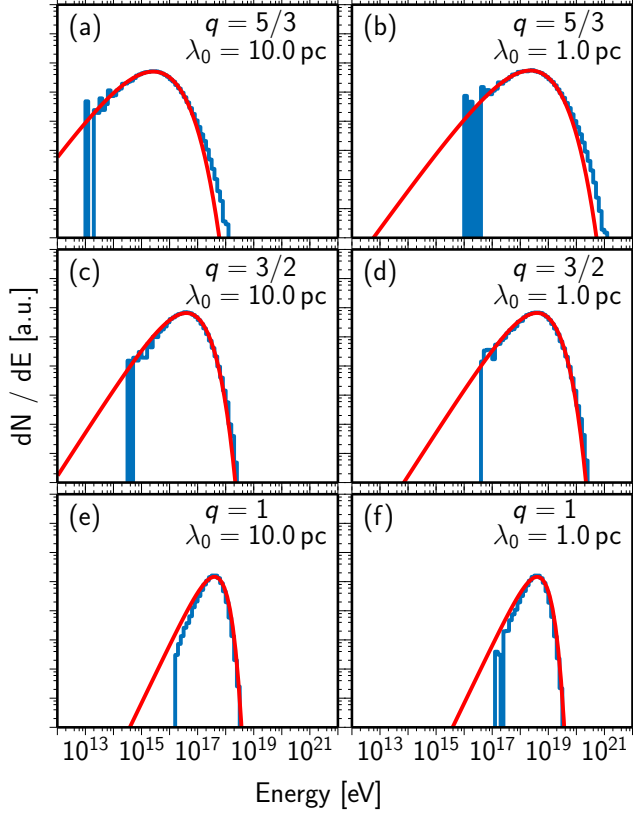


FIG. 1. Spectra obtained from the simulation of second order Fermi acceleration of protons with different values for the mean free path length parameter λ_0 and the turbulence spectrum q with $\beta = 0.05$. The red line shows a fit of eq. 2 to the data.

center of a spherical simulation volume of radius r . Every particle propagates linearly until it is scattered as described above. We stop the simulation when the particle leaves the simulation volume or is decelerated below a lower energy threshold E_{cut} . Injection energy and lower energy threshold are chosen as $E_{\text{inj}} = 100$ TeV and $E_{\text{cut}} = 1$ TeV as in CRPropa currently only the highly relativistic case $E \gg m_0 c^2$ can be calculated. Here, we further fix the radius of the simulation volume to $r = 100$ pc and investigated different values of λ_0 , β , and q only.

In figure 1 simulation results are shown for $q = 5/3$ corresponding to Kolmogorov turbulence, $q = 3/2$ corresponding to Kraichnan turbulence, and as an extreme case $q = 1$ corresponding to viscosity damping [14, 15] for two choices of λ_0 . As the particles are injected here in the center of the acceleration region, they cannot escape without being accelerated first because of their small mean-free path. This is different from shock acceleration where a fraction of particles is lost after each cycle. In the model discussed here, low energy particles can only escape from close to the border of the acceleration re-

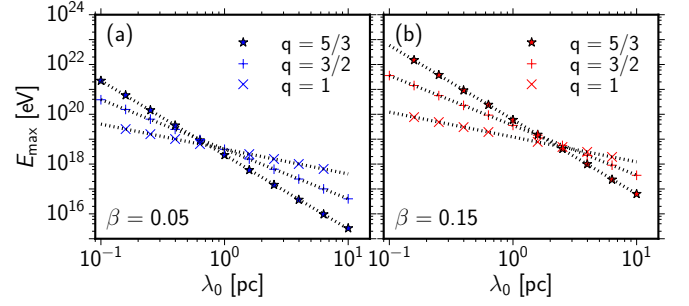


FIG. 2. Maximum of the source spectra E_{max} as function of the scatter length λ_0 for three choices of the turbulence spectrum q for (a) $\beta = 0.05$ and (b) $\beta = 0.15$. Colored markers are from a fit of eq. 2 to simulations as e.g. shown in figure 1; the dashed lines correspond to a power-law fit to the simulated points.

gion, while particles at the highest energies can escape from anywhere in the accelerating region. This effectively suppressed the naively expected power-law in the regime $\lambda_0 \ll r$, and the source spectrum can be reasonably well be described by a peaking distribution

$$\frac{dN}{dE} \propto E^{(3-q)} e^{-(E/E_0)^{(2-q)}}. \quad (2)$$

Only for larger λ_0 , or λ independent of the energy (both not shown here), the source spectra develop a power law tail.

For a given size of the accelerating region, the parameter E_0 of the distribution depends on the mean free path length λ_0 , the velocity of the scatter centers β , and the spectral index q of the magnetic turbulence. We found no dependency on the injection energy. From eq. 2 follows, that the position of the maximum of the distribution is given by

$$E_{\text{max}} = \left(\frac{3-q}{2-q} \right)^{\frac{1}{2-q}} E_0. \quad (3)$$

The dependency of E_{max} on λ_0 is shown in figure 2. A fit of a power-law $E_{\text{max}} \propto \lambda_0^{\left(\frac{1}{q-2}\right)}$ to the simulation perfectly describes the dependency. This is consistent with eq. 1, as this relation implies a linear dependency of E_{max} on the charge Z of the particles.

We fit the source spectrum given by eq. 2 to the energy spectrum and X_{max} distributions observed by the Pierre Auger Observatory [16, 17] accounting for propagation effects using simulations of UHECR propagation with the CRPropa software [13].

The 1D-simulations used here include energy losses and production of secondaries from pion-production, photo-disintegration, and electron pair production in the cosmic microwave background and infrared background of particles from sources up to 3 Gpc. Energy losses by adiabatic expansion of the universe and energy losses and

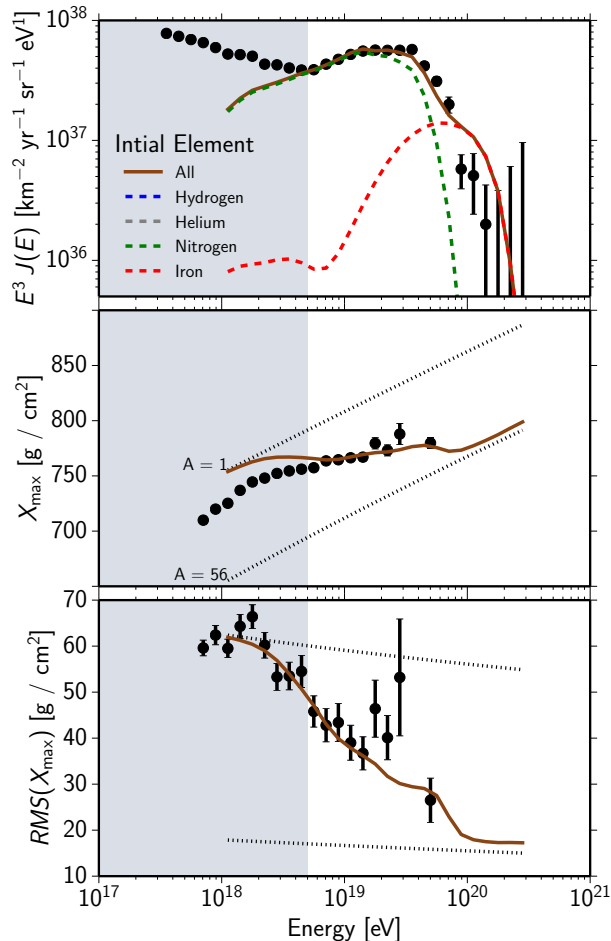


FIG. 3. Two parameter fit of the model described here to the data of the energy spectrum [16] (top), and the mean (middle) and root-mean-square (bottom) of the X_{\max} distributions measured with the Pierre Auger Observatory [17]. For the spectrum fit the contribution from the individual initial elements are marked as dashed lines. The gray marked area is not included in the fit.

secondary production from by nuclear decay are included as well. As a model for the infrared background we consider here only Gilmore2012 [18] and as model for the nuclear cross-sections only TALYS [19]. An overview of the effects of these models and simulation uncertainties is given in reference [20].

The fit-method used here is based on the method developed for the interpretation of the data of the Pierre Auger Observatory with power-law source spectra and an exponential cut-off [6, 21, 22]. To evaluate the effect of a source model on the observed cosmic rays, the energy and mass binned cosmic rays of a propagation simulation are re-weighted according to the source parameters. From the resulting weights for observed cosmic rays with energy and mass $(E, A)_i$ the spectrum and

X_{\max} distributions are calculated. For the calculation of X_{\max} from $(E, A)_i$ we use the usual parametrization based on the Gumble distribution and EPOS-LHC [23] as the hadronic interaction model [24]. The optimum set of source parameters is obtained by maximizing the likelihood of the observations using a Markov chain Monte Carlo code [25]. Differently from the original approach, here we use a Gaussian-based likelihood for the mean and RMS of the X_{\max} distribution.

The best fit is obtained for $\log_{10} Z E_{\max}/\text{eV} = 18.21 \pm 0.02$ and $q = 1.29 \pm 0.02$. With this fitting procedure, individual Markov Chains converge to different values for the individual element fractions while the values for q and E_{\max} are stable as indicated by a good Gelman-Rubin [26] statistic. The individual chains converge to different values for the individual elements, but the ratio of the Iron to Nitrogen fraction is well constrained in all Markov Chains to $f_{\text{Fe}}/f_{\text{N}} = (5.6 \pm 0.7) \cdot 10^{-4}$, and the values for Hydrogen and Helium are almost arbitrary due to the low maximum rigidity obtained in the fit. With these parameters, the expected values of the observables are shown together with the data in figure 3. For this four parameter fit to 36 data points we obtain a goodness-of-fit $\chi^2/\text{dof} = 58.8/32$.

The model presented here fits the data approximately as well as fits assuming power-laws [6]. This is not surprising, as from a mere technical point of view the spectrum proposed here is an inverted power-law with spectral index limited to $-2 \leq \gamma \leq -\frac{4}{3}$ and a slightly modified exponential cut off; results with $\gamma \leq 0$ have already been reported from fits of power-laws [6]. However, in the second order Fermi acceleration discussed here, this previously surprising parameter range is a natural consequence of the acceleration mechanism. The particular shape of the cut-off reduces the degeneracy between the parameters faced in fitting conventional power-law models. In particular, the cut-off expected here hardens the end of the spectrum compared to a naive exponential or broken-exponential cut-off; only for $q = 1$ the shape of the cut-off is identical to the common exponential cut-off. Consequently, the data above 5 EeV can be described with heavy primaries only and the fit becomes insensitive to the abundances of lighter elements.

Here we have considered only four elements, Hydrogen, Helium, Nitrogen, and Iron, where Nitrogen acts as a proxy for all elements with $2 < Z < 26$. Including more individual heavy elements in the fit will reduce the parameter E_{\max} further, as it allows a better description of the cut-off consistent with the ‘disappointing model’ [27]. The sources of extragalactic cosmic rays thus do not need to be surprisingly metal-rich as implied by power-law fits [28]. One can further speculate, that thus in this model the extragalactic sources of UHECR are also the origin of the strong light component below the ankle that have been recently measured [29, 30]. In addition to the inclusion of more elements, a detailed in-

vestigation of this requires the extension of the fit regime to lower energies and the inclusion of Galactic models in the fashion of [31] and is beyond the scope of this paper.

The fit results suggest that protons are accelerated on average to only approximately 1 EeV. Accelerating a thermal proton of 1 eV to 1 EeV with $\beta = 0.05$ in a second order Fermi process requires less than 12 500 scatter events. With the distance between interactions of $\lambda_0 = 1$ pc as used in the simulations above, the acceleration time t_{acc} is $t_{\text{acc}} \ll 50\,000$ yr and thus no principal constrain to the lifetime of many potential candidates for this mechanism as e.g. AGN jets. It is interesting to note, that the low-relativistic speeds of the scattering centers $\beta = 0.05$ required here corresponds to the Alfvén velocity expected in the outskirts of AGN jets (c.f. [11]). As the low maximum energy of 1 EeV also puts no severe constraints on the size and magnetic field of the source (c.f. [32]), such second order Fermi acceleration can be possible in many objects, as e.g. in jets of radio quiet AGNs. The consequently high number of sources contributing to the observed flux of UHECR is consistent with observational bounds on UHECR [33, 34] and neutrino sources [35].

With the model for cosmic ray acceleration presented in this paper we demonstrated, that the available observational data at the highest energies can be well interpreted without requiring a power-law for the energy spectrum at the sources of UHECR. In contrast to interpretations of the data with power laws as produced by shock acceleration, the best fitting parameters of the acceleration mechanism proposed here are not exceptional and do not imply an unexpected high abundance of heavy elements at the sources. The second order Fermi mechanism as discussed here does not suffer from an injection problem and is capable of accelerating particles from the thermal pool on sufficient time scales. It is consistent with a high number of sources and the non-observation of point sources. The required conditions for acceleration in the model discussed here, i.e. highly turbulent fields with low-relativistic velocities of the scatter centers, may be very abundantly found in the many astrophysical plasmas, indicating that UHECR sources are not exceptional but very common objects.

We gratefully acknowledge valuable comments to the manuscript from Roger Clay, Martin Erdmann, and David Walz. This research was funded by the European Research Council (ERC) under the European Union's Horizon 2020 research and innovation programme (grant agreement No 640130).

* tobias.winchen@rwth-aachen.de

[1] K.-H. Kampert and P. Tinyakov, *Comptes Rendus Physique* **15**, 318 (2014).

- [2] K. Kotera and A. V. Olinto, *Annual Review of Astronomy and Astrophysics* **49**, 119 (2011).
- [3] S. Colgate, *Physica Scripta* **T52**, 96 (1994).
- [4] P. Blasi, Invited Review Talk in UHECR2012 Symposium, CERN (2012).
- [5] A. Marcowith *et al.*, *Reports on Progress in Physics* **79**, 046901 (2016).
- [6] A. di Matteo for the Pierre Auger Collaboration, in *Proceedings of the 34th International Cosmic Ray Conference* (The Hague, The Netherlands, 2015).
- [7] D. Allard *et al.*, *Journal of Cosmology and Astroparticle Physics* **10**, 033 (2008).
- [8] R. Aloisio, V. Berezhinsky, and P. Blasi, *Journal of Cosmology and Astroparticle Physics* **2014**, 020 (2014).
- [9] M. Unger, G. R. Farrar, and L. A. Anchordoqui, *Physical Review D* **92**, 123001 (2015).
- [10] E. Fermi, *Physical Review* **75**, 1169 (1949).
- [11] S. O'Sullivan, B. Reville, and A. M. Taylor, *Monthly Notices of the Royal Astronomical Society* **400**, 248 (2009).
- [12] J. Scalzo and B. G. Elmegreen, *Annual Review of Astronomy and Astrophysics* **42**, 275 (2004).
- [13] R. Alves Batista *et al.*, *Journal of Cosmology and Astroparticle Physics* **05**, 038 (2016).
- [14] J. Cho, A. Lazarian, and E. T. Vishniac, *The Astrophysical Journal* **595**, 812 (2003).
- [15] J. Cho, A. Lazarian, and E. Vishniac, in *Turbulence and magnetic fields in astrophysics*, edited by E. Falgarone *et al.* (Springer, Heidelberg, 2003) pp. 56–100.
- [16] I. Valio for the Pierre Auger Collaboration, in *Proceedings of the 34th International Cosmic Ray Conference* (The Hague, The Netherlands, 2015).
- [17] A. Aab *et al.* (Pierre Auger Collaboration), *Physical Review D* **90**, 122005 (2014).
- [18] R. C. Gilmore *et al.*, *Monthly Notices of the Royal Astronomical Society* **422**, 3189 (2012).
- [19] A. J. Koning, S. Hilaire, and M. C. Duijvestijn, *AIP Conference Proceedings* **769**, 1154 (2005).
- [20] R. Alves Batista *et al.*, *JCAP* **1510**, 063 (2015).
- [21] D. Walz, Ph.D. thesis, RWTH Aachen University (in preparation).
- [22] The Pierre Auger Collaboration, in preparation.
- [23] K. Werner, I. Karpenko, and T. Pierog, *Physical Review Letters* **106**, 122004 (2011).
- [24] M. De Domenico *et al.*, *JCAP* **1307**, 050 (2013).
- [25] A. Patil, D. Huard, and C. Fonnesbeck, *Journal of Statistical Software* **35**, 1 (2010).
- [26] A. Gelman and D. B. Rubin, *Statistical Science* **7**, pp. 457 (1992).
- [27] R. Aloisio, V. Berezhinsky, and A. Gazizov, *Astroparticle Physics* **34**, 620 (2011).
- [28] D. Boncioli, A. di Matteo, and A. Grillo for the Pierre Auger Collaboration, in *Proceedings of the Cosmic Ray International Seminar (CRIS)* (Gallipoli, Italy, 2015).
- [29] A. Porcelli for the Pierre Auger Collaboration, in *Proceedings of the 34th International Cosmic Ray Conference* (The Hague, The Netherlands, 2015).
- [30] S. Buitink *et al.*, *Nature* **531**, 70 (2016).
- [31] S. Thoudam *et al.*, *Astronomy & Astrophysics* **under review** (2016), arXiv:1605.03111.
- [32] A. M. Hillas, *Annual Review of Astronomy and Astrophysics* **22**, 425 (1984).
- [33] P. Abreu *et al.* (Pierre Auger Collaboration), *JCAP* **1305**, 009 (2013).
- [34] A. Aab *et al.* (Pierre Auger Collaboration), *The Euro-*

pean Physical Journal C **75**, 269 (2015).

[35] M. G. Aartsen *et al.* (IceCube), The Astrophysical Journal **under review** (2016), arXiv:1609.04981.